Radiomics-Based Liver Tumor Classification Using Floating Forward–Backward Feature Selection and a Modified VGG19 Deep Network

[1]Anjana V T, [2]Dr. Tajunisha N
[1]Ph.D Research Scholar, [2]Professor
[1] Department of Computer Science,
[1] Sri Ramakrishna College of Arts and Science for Women, Coimbatore, Tamil Nadu, India

Abstract

Liver cancer is one of the leading causes of cancer mortality in the world and to improve the survival of patients and management of the disease, proper and early identification of liver tumor is important. Medical imaging procedures such as CT scans are popular in the diagnosis of tumors the are time-saving, but can be manualized, which will tend to introduce variation in clinical decisions. Based on this, computer-aided diagnostic systems based on the Artificial Intelligence (AI) method of automation have become more popular as far as diagnostic accuracy is regarded. This research will mainly focus on developing an efficient model of liver tumor detection and classification to remove redundant imaging features and improve prediction accuracy. To achieve this, the proposed strategy will integrate radiomics feature extraction with Floating Forward and Backward Selection (FFBS) algorithm to identify the most and least relevant features respectively. This subset of features is optimized (VGG19 based) and inputted into a Modified Deep Convolutional Neural Network (DCNN) to have the tumors correctly classified. Furthermore, the Grad-CAM representation is applied to visualize the locations of the tumors and improve the model interpretability. The trial results of liver CT picture indicate that the proposed structure generates a superior performance as compared to the existing strategies where the classification accuracy stands at 97.70 %. These results confirm that the mixture of the feature optimization by the use of FFBS and the Deep Learning (DL) classification can be regarded as a reliable and consistent tool to diagnose liver tumors automatically and support the improvement of clinical judgment.

Keywords: Deep Convolutional Neural Network, Feature Selection, Floating Forward Backward Selection, Liver Tumor Detection, Radiomics Features, VGG19 Architecture

How to cite this article: Anjana VT, Tajunisha N. Radiomics-Based Liver Tumor Classification Using Floating Forward–Backward Feature Selection and a Modified VGG19 Deep Network. Int J Drug Deliv Technol. 2026;16(76s): 1132-1148. DOI: 10.25258/ijddt.16.76s.101

1. Introduction

Liver cancer is one of the primary causes of cancer-related mortality across the entire globe and the discovery of liver tumors at early stages is the secret of the better survival and treatment of the cancer patients. The common types of medical imaging techniques such as CT, MRI, and histopathology imaging are used as imaging techniques to detect liver abnormalities and the areas of the tumor. However, these images are time consuming to be analyzed by radiologists manually, and such a technique involves the ability of the radiologists which lead to the inconsistency of the diagnosis. Recent advances in Artificial Intelligence (AI), Machine Learning (ML) and Deep Learning (DL) have enabled the analysis of medical images in an automatic way to improve the accuracy and efficiency of the diagnostic outcome. Though, such concerns as heterogeneity of tumors, various image appearances and redundant imaging features still remain and disrupt the reliable detection and classification of liver tumors.

These problems have been attempted to be resolved through different studies using different AI and imaging modalities. As an example, the classification and prediction of mutation of liver cancer by H&E images based on deep learning-based histopathology analysis have been conducted [1]. Attention-based optimization algorithms have also been achieved to predict liver tumors and to further increase the feature learning as well as the classification accuracy [2]. Clinical research has been carried out to determine the relationship between the tumor characteristics and the immune cells in liver tissues to gain a better insight into the progression of the tumor [3]. In addition to this, metabolic pathways involving liver tumorigenesis have been discussed in glycogen storage disorders on biological research [4]. The imaging diagnostic techniques have also been used to make comparisons between CT and MRI techniques of establishing precise preoperative evaluations of tumors in the liver [5]. Bayesian optimized probabilistic neural networks are ML tools that have been proposed in tumor classification [6]. The AI models of confocal fluorescence imaging have been analyzed to distinguish the nucleus of cancerous cells in hepatocellular carcinoma [7]. DL based detection architectures with multi scale

feature fusion and convolutional architecture have shown promising outlooks in the localization of tumor regions in liver images [8]. Biosensor based methods have also been used in detection of liver tumor biomarkers using detection methods that are based on biosensors at high sensitivity [9]. Furthermore, CT-based DL architectures have been created to identify and outline tumors within clinical imaging information based on artificial intelligence [10]. It has been proposed that enhanced optical probes can be used to identify tumors and liver abnormalities by performing multiple tasks [11], but enhanced computer-aided diagnostic models of PSO-PSP-Net and InceptionV3 have been used to improve tumors in liver CT scans [12]. However, the majority of these methods are restricted by such aspects as the complexity of calculations, dependence on big data, and inability to use the due to duplications of feature extraction. In this respect, the given research can contribute to the elimination of these issues by implementing a radiomics-based feature selection algorithm known as Floating Forward and Backward Selection (FFBS) algorithm and a Modified Deep Convolutional Neural Network (DCNN) with the VGG19 architecture. The selected framework will also strive to extract the most informative radiomics features of liver CT scans, remove redundant data, and improve the accuracy of tumor classification through the assistance of feature learning and prediction through the assistance of the DL.

- To enhance the vision of liver tumors detection method through the combination of radiomics feature extraction and the use of the DL techniques.
- To eliminate unnecessary and redundant imaging characteristics with FFBS algorithm.
- To establish an effective liver tumor classification system with the help of a Modified DCNN on the VGG19 structure.
- To improve the interpretability and reliability of the models using Grad-CAM based tumor region visualization.
- To outperform the current methods in accuracy, precision, recall, and F1-score, and specificity.

Organization: Section 1 will be the introduction section, and it will include the background section, problem definition, related work, and the proposed approach, and Section 2 will be the background research of the liver tumor detection with the assistance of the ML and DL methods. Section 3, details the proposed methodology including the dataset, radiomics mechanism using the FFBS algorithm and liver tumor classification using a modified DCNN, and based on VGG19, and Section 4, contains the research findings and performance results, and Section 5, includes the conclusion of the research and the key findings and future directions of the research.

2. Background Study

Ma et al. (2024) [13] presented a Transformer Dense Center Network (TDCN) to detect liver tumors with dense connections and transformer attention to enhance the representation of features and localization accuracy. Validation on a wide range of multi-centers and computation complexity were yet to be fully validated and experimental evaluation indicated a higher detection precision and robustness over conventional CNN-based models.

In Kan et al. [14] proposed a DL based model that can detect motions of liver tumours using fiducial markers in kilo volt X-ray to improve radiotherapy delivery. The reliance on implanted markers and limited clinical-scale validation was a sign of limitation; however, the evidence demonstrated appropriate performance in motion tracking, which can be utilized in real-time radiotherapy.

Ma et al. (2022) [15] determined the tumour boundary in metastatic liver disease with the aid of 2D multibreath-hold susceptibility-weighted imaging to enhance the delineation of the lesion. Limitations to selected MRI protocols and a lack of automation indicated gaps in the research, and the results indicated an enhanced visualization of boundaries in comparison with the research imaging sequences.

The research by Shi et al. (2023) [16], proposed a four-fold signal amplification self-powering amol-level liver cancer tumor marker detection MoS2@C hollow nanorods-based DNA hexahedral framework biosensor. Clinical validation scale and practical deployment potential was still a limitation, but analytical experiments were ultra-sensitive in detection, and very specific.

Zhao et al. (2021) [17] introduced a joint adversarial adversarial learning system to segment and detect liver tumors simultaneously based on multi-modality non-contrast MRI images. It was observed that little room was covered on contrast-enhanced modalities and recreational requirements, whilst outcomes were reported of improved segmentation precision and heightened generalization achievement.

Yang et al. (2022) [18] used a multi-scale convolutional network with feature alignment to detect pathologic liver tumor, as it can identify hierarchical spatial characteristics. The limitation

of diversity and interpretability of data sets and evaluation and analysis of the performance demonstrated better detection rates than baseline CNN models.

Aslam et al. (2021) [19] adopted a CNN Residual U-Net (ResUNet) architecture with a combination of residual learning and U-Net segmentation approach, in which liver and tumor detection are automated. Sensitivity to noise and lack of cross-dataset validation were research gaps, and the results of the research showed high measures of segmentation accuracy and improved F1-score.

In comparative study, Kose et al. (2020) [20] used intraoperative liver tumor detection techniques, which are indocyanine green fluorescence and laparoscopic ultrasound, in a surgical setting. There were some limitations in the sample size and reliance on operator expertise but comparative analysis showed that there were complementary detection advantages with significant sensitivity differences.

Abdelrahim et al. (2022) [21] studied the viability of tumor-guided circulating tumor DNA-based predictive testing to identify the recurrence of hepatocellular carcinoma following liver transplantation. The cohort size was small and the initial analysis was done in the feasibility of the research itself which demonstrated the limitations and the results were promising in the sensitivity of detecting early recurrence.

Table 1: Background Research of Recent DL Methods to analysis liver tumors

Author (Year)	Concept	Methods Used	Research Gap	Limitations	Results
Jameel & Amin (2026) [22]	Unified liver tumor classification and segmentation	Shifted window transformer network with incremental learning	Limited unified frameworks combining classification and segmentation were identified	High computational cost and dependency on large annotated datasets were observed	Improved segmentation accuracy and classification performance were achieved with better generalization
Wu et al. (2026) [23]	Liver tumor segmentation using feature fusion Kolmogorov–Arnold network	FFK-Net with feature fusion strategy	Lack of nonlinear functional approximation in segmentation models was reported	Model complexity and training instability were noted	Enhanced Dice score and boundary precision were obtained compared to baseline CNN models
Spinczyk et al. (2026) [24]	Mixed-reality navigation for liver tumor ablation	Image-guided mixed-reality system evaluation	Limited integration of MR systems in percutaneous ablation was observed	Initial pilot evaluation with small clinical validation was conducted	Improved navigation accuracy and procedural guidance feasibility were demonstrated
Hossain (2026) [25]	Precise liver and tumor segmentation in CT	EfficientNet-based multi-scale feature fusion with hybrid spatial-channel attention	Insufficient attention-based feature refinement in CT segmentation was identified	Performance sensitivity to varying CT acquisition parameters was noted	Higher segmentation accuracy and improved IoU values were achieved

Bal et al. (2026) [26]	Robust 3D liver tumor segmentation	D33D-Net with dynamic deformable dual-pathway and handcrafted features	Limited 3D adaptive deformable learning integration was reported	Increased training time and computational resource requirement were observed	Superior volumetric Dice score and robust cross-dataset performance were achieved
Ma et al. (2026) [27]	Multi-scale spatial-frequency feature enhancement	MSFFE-Net for segmentation	Insufficient spatial-frequency feature exploitation was identified	Reduced performance on very small lesions was observed	Improved segmentation precision and boundary delineation metrics were achieved
Gowda &Manjunath (2025) [28]	Automatic liver tumor classification	UNet 70 DL model	Limited classification-specific U-Net adaptations were identified	Restricted dataset diversity was observed	High classification accuracy with improved F1-score was achieved
Arora et al. (2025) [29]	Liver tumor and vein segmentation	DL with transfer learning models	Limited multi-structure segmentation framework	Transfer learning dependency on pretrained weights was observed	Improved segmentation accuracy for tumors and vascular structures was achieved
Rahman et al. (2025) [30]	CT and MRI liver tumor volumetric segmentation	Ensemble ResUNet-Inception V4 model	Need for multi-modality ensemble approaches was highlighted	Increased ensemble complexity and inference time were observed	High Dice coefficient and improved robustness across CT and MRI datasets were achieved

The table 1 provided above is the systematic comparison of the recent researches centered on the liver tumor detection and the image-guided intervention with the help of high-quality ML and DL algorithms. It stresses the fundamental idea, the approaches like transformer networks, CNN-based models, ensemble learners, attention mechanisms, and hybrid 3D architectures, as well as research gaps and limitations have been identified.

Research Gap

- The current liver tumor detention schemes usually have redundant feature acquisition, which lowers the classification precision.
- Most DL models are computationally expensive and need massive sized annotated datasets which is a drawback.
- The existing methods are limited in terms of the optimization of features and interpretability, which influence the effective classification of a tumor.

3. Proposed Methodology

This section will involve the proposed liver tumor examination framework which will consist of the radiomics based picture feature extraction and the Modified DCNN classification. The overall architecture, workflow and the noteworthy equations and the pseudocodes are also presented to show how the FFBS algorithm takes

advantage of the feature subsets optimally, and how VGG19-based DCNN can be used to classify tumors adequately. The current section also brings about a more detailed insight on the methodology, which aims at combining feature selection, DL, and the performance measure to be in a place to spring liver tumor detection.

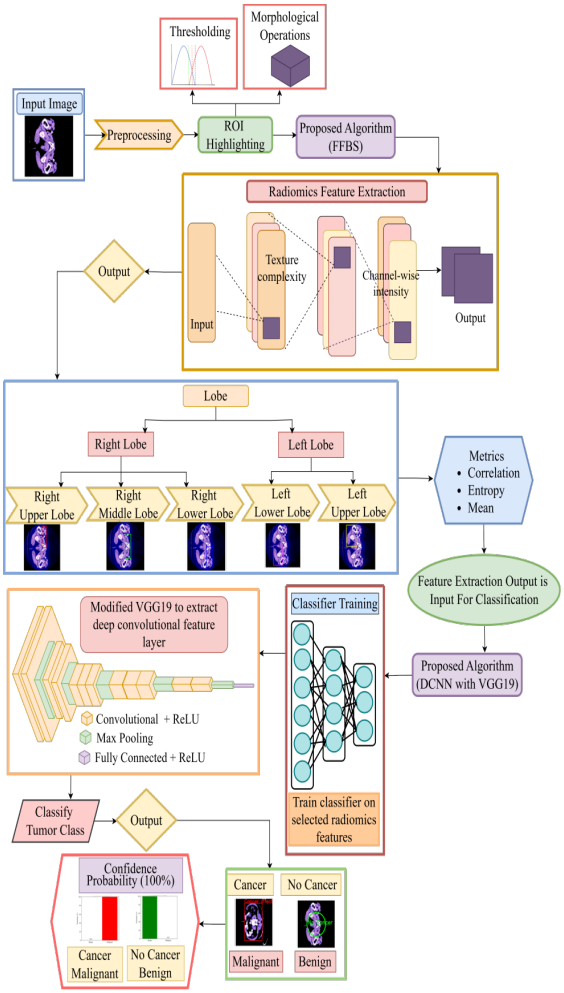

Figure 1: Architecture composition of the proposed Radiomics and modified DCNN (VGG19) model to detect liver tumors

Figure 1 above, the entire process of the flow of the proposed liver tumor detection system 1 will comprise preprocessing of medical images and identification of ROI through thresholding and morphological processing and then the extraction and selection of the radiomics with the help of the FFBS algorithm. A chosen set of features is then trained with a classifier and learned deep features with a Modified VGG19-based DCNN to provide the classification of tumor as benign or malignant with a confidence probability.

3.1 Dataset

This data is on contrast enhanced-abdominal CT scans of liver tumor segmentation, both volumetric and liver and tumor region ground truth masks, which was initially published in the Liver Tumor Segmentation (LiTS) challenge, and the dataset is available at https://www.kaggle.com/datasets/harshwardhanbhangale/lits-dataset. It has hundreds of high resolution CTs slices labeled by professionals, and of varying shapes, sizes and appearance of the tumors of various patients. The open-source dataset is the one that can be transferred to medical imaging sphere and be trained and evaluated on the frameworks of segmentation and classification.

3.2 Radiomics Feature Extraction using FFBS

Radiomics Feature Extraction attempts to identify features of an imaging that are most informative to remove any redundant or irrelevant features to improve upon classification performance. FFBS algorithm starts with an empty set of features and continues to add features one at a time which gives the greatest increase in model accuracy (forward step) . It will test the features it has added in the previous addition and remove those whose removal will benefit its performance (backward step). Such floating proceeds until can add no more to it, until are adding features that will be useful and removing those that will not add to it. The FFBS is preferable as it does not experience local minima issue of simple forward or backward selection and also gives a small and optimal feature subset. The selected features are then passed on to the classifier that removes the computational cost as well as the accuracy of the classifying tumours.

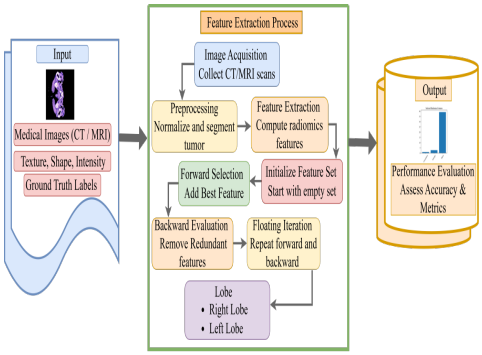

Figure 2: Radiomics-Based Feature Extraction Liver tumor

In the figure 2 above, the overall workflow of the proposed feature extraction system of liver tumor is presented in the aid of the CT/MRI images. Since the input is already given, medical images are first given, and next, preprocessing and radiomics feature extraction are then done. The floating feature selection algorithm is used by repetition of forward selection and

backward elimination steps to remove the redundant features and get the optimal set of features that is then tested using performance measures such as accuracy and other measures used in classification.

$$S_{t+1} = S_t \cup \{f_i\}, \quad f_i = \arg\max_{f \in F \setminus S_t} Accuracy(S_t \cup \{f\}) \tag{1}$$

In equation 1 is used to denote that S_t is a current collection of chosen features at the iteration t, F is a complete group of available features, f_i Feature that, on inclusion, will maximize the accuracy, S_{t+1} is an updated group of features that incorporates the newly chosen feature. In each iteration include the feature in the remaining set with the highest model improvement.

$$S_{t+1} - S_t \backslash \{f_j\}, \quad f_j - \arg\max_{f \in S_t} Accuracy(S_t \backslash \{f\}) \tag{2}$$

In equation 2 denotes that f_j is a feature whose deletion maximally enhances the model, $S_t \backslash \{f_j\}$ is a feature set following deletion f_j, S_{t+1} is an updated set following backward deletion. Add features to minimise inaccurate features to narrow the feature set.

$$Accuracy(S) = \frac{TP+TN}{TP+TN+FP+FN} \tag{3}$$

In equation 3 is an illustration that TP, TN represents a correctly predicted positive and negative instance, FP, FN represents an incorrectly predicted positive and negative instance. Measures the ability of the current set of features to be accurate predictors of outcomes

$$C(f) = Accuracy(S \cup \{f\}) - Accuracy(S) \tag{4}$$

In equation 4 denotes that $C(f)$ is a contribution of feature f to the improvement in accuracy, $S \cup \{f\}$ is a subset of features following addition of f. Lists the performance of the model improvement as a result of a particular feature

$$\Delta Accuracy < \in \tag{5}$$

In equation 5 means that $\Delta Accuracy$ is the difference between accuracy with the addition/removal of a feature, $\in$ is a pre-set small value to prevent iterations. Terminate the algorithm when the changes in the features do not increase the accuracy significantly anymore.

$$S^* = \arg\max_{S \subseteq F} Accuracy(S) \tag{6}$$

In equation 6 corresponds to the fact that S^* is an optimal subset of features that maximizes the accuracy of a model, $S \subseteq F$ represents a candidate subset of the entire set of features. Takes steps to ensure the end chosen subset is as accurate as possible.

$$Redundancy(f_i, f_j) = 1 - |Corr(f_i, f_j)| \tag{7}$$

Where in equation 7 is defined as $Corr(f_i, f_j)$ is a correlation between features f_i and f_j, $Redundancy(f_i, f_j)$ measures the uniqueness; the larger the value the lower the redundancy. It is important to avoid the selection of very highly correlated features to eliminate overlaps in the subset.

Pseudocode 1: Radiomics Feature Extraction using FFBS

```
Input:
F → Set of all extracted radiomics features
Classifier → ML model to evaluate feature subsets
AccuracyThreshold → Minimum improvement required to continue
Initialize S_optimal = empty set
Set improvement = True
While improvement is True:
    improvement = False
    # ----- Forward Step -----
    For each feature f in F \ S_optimal:
        temp_set = S_optimal ∪ {f}
        Evaluate classifier performance on temp_set
        Record accuracy
    End For
```

```
    f_best = feature with highest accuracy improvement
    If accuracy improvement > AccuracyThreshold:
        Add f_best to S_optimal
        improvement = True
    End If
    # ----- Backward Step -----
    For each feature f in S_optimal:
        temp_set = S_optimal \ {f}
        Evaluate classifier performance on temp_set
        Record accuracy
    End For
    f_remove = feature whose removal improves accuracy
    If removal improves accuracy > AccuracyThreshold:
        Remove f_remove from S_optimal
        improvement = True
    End If
End While
Return S_optimal
Output:
S_optimal → Optimal subset of features selected
```

In the pseudocode 1, the starting feature set is taken as empty and a forward step is repeated over the feature set and the feature that best increases the accuracy of the classifier is added. Every addition is followed by a backwards step deciding whether or not any existing feature can be removed and improve the performance further, discarding the non-contributing features. This is repeated until no significant progress is made to yield an optimal set of radiomics features to classify the tumor correctly.

3.3 Liver Tumor Classification using Modified DCNN with VGG19

A Modified DCNN based on VGG19 architecture, a deep model, is used to classify liver tumor, as it is an effective model used to extract image features. The network is then optimized on the liver tumor data by manipulating the weights of the already trained layers to conform better to the data and learn domain specific patterns. The input to the network is the set of radiomics features that have been chosen in the previous step and filters out noise and highlights the most informative features. The model transforms the input by going through several convolutional, activation and pooling layers and obtaining hierarchical features which convey tumor texture, shape as well as intensity variations. These features are then added in fully connected layers to generate discriminative representations to classify it. Through training, the network is used to reduce a loss function in order to maximize prediction accuracy. The outcome of the research should be proper categorization of liver tumors into the categories, enhancing clinical decision-making and machine analysis.

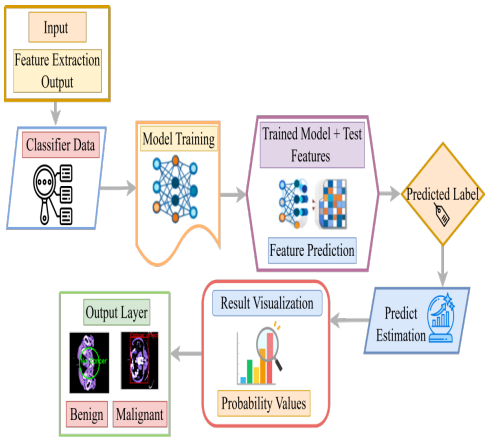

Figure 3: The Proposed DL-Based Liver Tumor Classification Framework Workflow

Figure 3 above shows a general layout of the proposed classification scheme of liver tumor. The input to the classifier is the feature extraction output and then training and prediction on the trained model is done using test features. Lastly, the system produces the predicted labels (benign or malignant) and probability-based visualization of the results to aid in proper diagnosis of the tumor.

$$F_l^K = \sigma\left(\sum_i F_{l-1}^i * W_l^{i,k} + b_l^k\right) \quad (8)$$

In equation 8 is the representation that F_l^K is an output feature map in layer l of filter k, F_{l-1}^i is an output feature map in layer i, $W_l^{i,k}$ is a convolution kernel (weights) between input i and filter k, b_l^k is an abias of filter k in layer l, and used is the activation function (e.g., ReLU). Learnable filters that can extract spatial patterns of input feature maps are used in order to capture tumor features.

$$P_l^k = maxpool\left(F_l^k\right)$$
(9)

In equation 9 indicates that P_l^k is a pooled feature map (down sampled), F_l^k is a convoluted layer input feature map. Find a space-reduction method that will not lose significant features, and the model would be resistant to translations.

$$x = Flatten(P_L)$$
(10)

In equation 10 means that PL is a given output of the final pooling layer, x is one-dimensional array of all features of fully connected layers. Transform many dimensional features maps into a single dimensional feature that is amenable to classification.

$$y = \sigma(W_x + b)$$
(11)

Equation 11 is a depiction of the fact that W_x is a weight matrix in the fully connected layer, b is a bias vector in the layer, y is an output activations (pre-softmax). Forms discriminative features of extracted features to classify tumors

$$\hat{y}_i = \frac{e^{y_i}}{\sum_j e^{y_j}}$$
(12)

In equation 12 symbolizes the fact that $\hat{y}_i$ is a predicted probability of class i, and y_i is a fully connected layer output of class i. The predictions on the network are converted into the probabilities of various tumors

$$L = -\sum_i y_i log(\hat{y}_i)$$
(13)

The equation 13 indicates that y_i is a true label (one-hot encoded) of class i, and $\hat{y}_i$ is a predicted probability of class i. The guide learning is the comparison of the predicted probabilities with the actual labels.

$$W \leftarrow W - \eta \frac{\partial L}{\partial W}$$
(14)

The equation 14 shows that W is layer weights which is being updated, η is a learning rate which steps the size of update, L is a loss function (cross-entropy). Tilts weights and adjusts in order to reduce loss and increase model accuracy.

$$Accuracy = \frac{Number\ of\ Correct\ Predictions}{Total\ predictions}$$
(15)

In equation 15 is an indicator that $Correct\ Predictions$ is the count of accurately-classified tumor specimens, $Total\ predictions$ is the aggregate count of tumor samples that were analyzed. Test the trained DCNN using a consideration of the classification of the tumors.

Pseudocode 2: Liver Tumor Classification using Modified DCNN (VGG19)

Input:

X_train → Training data (selected radiomics features)

Y_train → Training labels (tumor classes)

X_test → Testing data

Y_test → Testing labels

Pretrained_VGG19 → Pre-trained VGG19 model

Epochs → Number of training iterations

LearningRate → Learning rate for optimizer

Step 1: Load pre-trained VGG19 model

Model = Load_Pretrained_VGG19(Pretrained_VGG19)

Step 2: Modify the network

Remove original fully connected layers from Model

Add new fully connected layers suitable for liver tumor classification

Add output layer with number of neurons = number of tumor classes

Apply softmax activation to output layer

Step 3: Prepare data

X_train, X_test = Normalize_Features(X_train, X_test)

Y_train, Y_test = One_Hot_Encode(Y_train, Y_test)

```
# Step 4: Fine-tune the network
For epoch = 1 to Epochs:
    For each batch in X_train:
        Forward propagate batch through Model
        Compute loss between predicted and true labels
        Backpropagate loss to update weights
    End For
End For
# Step 5: Evaluate the trained model
Y_pred = Model_Predict(X_test)
Accuracy = Compute_Accuracy(Y_test, Y_pred)
Return Model, Y_pred, Accuracy
Output:
Model → Trained Modified DCNN
Y_pred → Predicted tumor classes for X_test
Accuracy → Classification accuracy
```

Pseudocode 2 in the above code starts with the initialisation of an already trained VGG19 model and reconfiguring the fully connected layers to accommodate liver tumor classes. It then normalizes the selected radiomics features, imparts the network through forward and back propagation in multiple epochs and enhances weights in order to maximize classification. Finally, the trained model will give the prediction of the tumor classes on the test, and therefore determine the accuracy hence providing an effective classifier on the identification of liver tumor.

4. Result and Discussion

The results and discussion section show the experimental results that were achieved in the proposed liver tumor detection framework. The experiments and performance analysis were done in the Python programming environment where feature extraction, feature extraction between the FFBS algorithm was done, and classification by the use of the Modified DCNN (VGG19) model was done. Extraction of radiomics of the liver CT images was performed and utilized in training and testing the proposed model. The results obtained have shown better accuracy, precision, recall, F1-score, and specificity than the current methods.

4.1 Feature Extraction

Feature Extraction is the process of identifying and deriving meaningful quantitative features from medical images to represent important tumor characteristics such as texture, shape, and intensity for accurate analysis and classification.

Table 2: Liver Image Selected Texture Features

Feature No	Feature Name
1	Correlation
2	Entropy
3	Mean

The table 2 above has included the important features Correlation, Entropy and Mean that have been selected to proceed with the analysis of liver CT images.

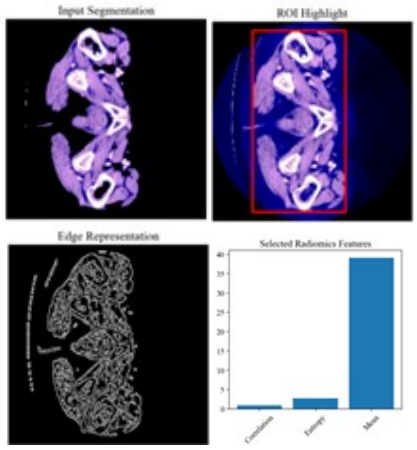

Figure 4: The Radiomics Feature Extraction Workflow on the Analysis of Liver Tumors

The figure 4 above shows the step-by-step process of the radiomics feature extraction of liver CT images that includes input segmentation, Region of Interest (ROI) highlighting, and edge representation of the tumor region. Radiomics features extracted are then quantified and visualized and later utilized in the extraction of features and classification of tumors.

4.1.1 Right Lobe

The largest hepatic lobe and most frequently identified location of liver tumours are in the right lobe of the liver because it is larger and has more blood of supply.

Table 3: Distribution of Detected Regions in the Input images Lobe-wise

Image	Input Image	Right Upper Lobe	Right Middle Lobe	Right Lower Lobe
1	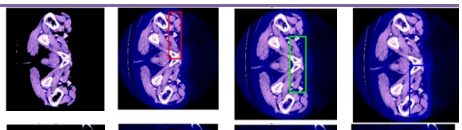			
2	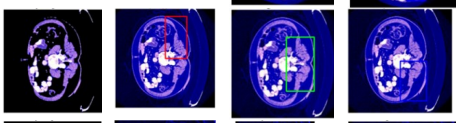			
3	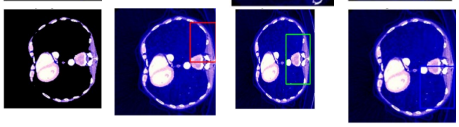			

The table 3 above shows the analysis of input images concerning the various anatomical lobes, namely, the Right Upper Lobe, Right Middle Lobe and right lower Lobe. It emphasizes the spread of the identified regions or observations across these lobes in relation to both input images, which allows the comparison of the patterns of a particular lobe.

4.1.2 Left Lobe

The left lobe of the liver is inferior to the right one but has a great role in the valuation of liver tumors because the tumors found in this area might affect other vascular and biliary liaison structures.

Table 4: Left Lobe Region Analysis of Liver Tumor on the Input Images

Image	Input Image	Left Upper Lobe	Left Lower Lobe
1	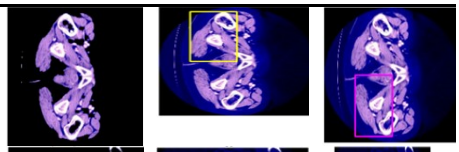		
2	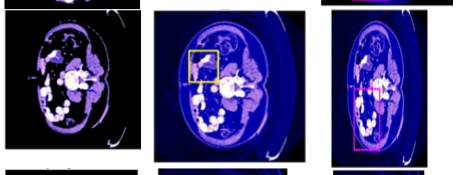		
3	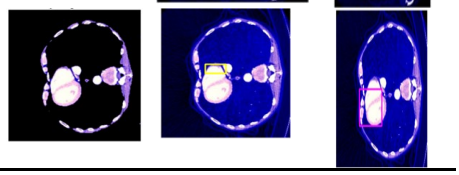		

The table 4 above shows the analysis of input images based on the regions of the liver that are on the left such as the Left Upper Lobe and Left Lower Lobe. It depicts the distribution of tumor presence or regions detected in each of the anatomical sections in each image under analysis.

Table 5: Extraction of Texture Features of Liver images

Image No	Energy	Contrast	Correlation	Mean	Std Dev	Entropy
1	0.732258	435.683548	0.957600	39.065613	71.579792	2.742385
2	0.806497	799.046109	0.908708	28.136642	66.048056	1.996247
3	0.842919	477.156480	0.956358	29.402237	73.815485	1.613558

The table 5 above indicates major texture characteristics that are obtained after processing liver CT images such as Energy, Contrast, Correlation, Mean intensity, Standard Deviation, and Entropy. These characteristics aid in quantification of the changes of texture and intensity in the images which proves useful in identifying patterns related to liver abnormalities.

Table 6: Comparative Results of the Performance of Feature Extraction Methods on FFBS with Liver tumor analysis

Methods	Accuracy (%)	Precision (%)	Recall (%)	F1-Score (%)
CNN [1]	88.60	87.90	86.80	87.30
Attention Mechanism [2]	90.20	89.40	88.70	89.00
PNN [6]	91.30	90.50	89.80	90.10
PSPNet [12]	92.70	91.90	91.20	91.50
TDCN [13]	93.60	92.80	92.10	92.40
Proposed Algorithm (FFBS)	95.40	93.30	92.20	92.10

The table 6 above shows the performance comparison of various ML and DL algorithms with the proposed FFBS algorithm. The evaluation measures demonstrate that the proposed approach is more accurate and has better classification capability than the current ones.

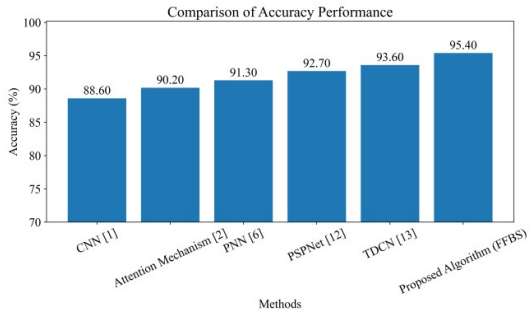

Figure 5: Comparison of Feature Extraction Methods Accuracy

Above figure 5 presents the accuracy of various feature extraction and classification models of CNN, Attention Mechanism, PNN, PSPNet, TDCN, and the proposed FFBS algorithm. The various methods are plotted on the X-axis and the accuracy (%) on the Y-axis, which shows that the proposed FFBS method is better at enhancing the performance of the classification due to the potential to identify the most useful radiomics features.

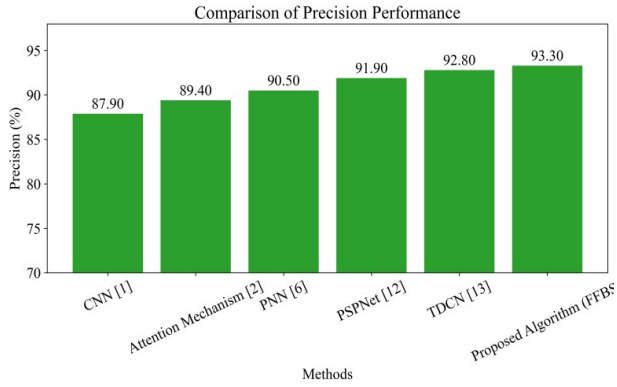

Figure 6: Precision Comparison of Feature Extraction Methods

In figure 6 above present the accuracy tables of different models that have been used in features extraction and classification showing the accuracy of each model in identifying positive tumor samples. The X-axis containing the compared algorithms and the Y-axis which is the precision (%) are highlighting that the proposed FFBS algorithm lowers the false positive predictions and increases the reliability of detection.

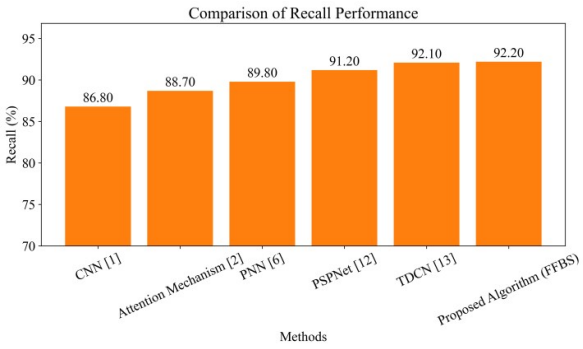

Figure 7: Recall Comparison between Feature Extraction Methods

In figure 7 above displays the recall performance of various algorithms, which is the performance of each algorithm in detecting actual tumors in the dataset correctly. The X axis denotes the classification methods whereas the Y axis denotes the recall (%) which demonstrates that the proposed FFBS method is more effective in detection as it reduces the cases of missed tumors.

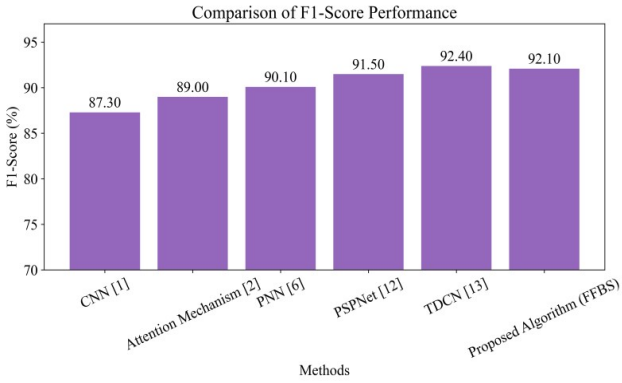

Figure 8: Comparison of F1-Score of Feature Extraction Methods

Above figure 8 compares the values of F1-Score of various methods which are a balanced measure of the precision and recall to the task of classification. The X-axis indicates the compared algorithms, and the Y-axis corresponds to the F1-Score (%) showing that the proposed FFBS algorithm is performed much more successfully in terms of its overall functionality in terms of feature extraction and accuracy in the classification.

4.2 Classification

This section outlines the procedure of categorizing the computed liver CT images as cancerous and non-cancerous based on the proposed Modified DCNN model.

Table 7: Cancer Detection and Confidence Probability Analysis

Cancer Affect		
Input Image	**Tumor Highlight/ Cancer Status**	**Confidence Probability (100%)**
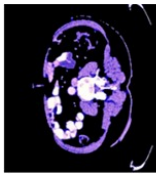	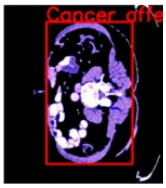	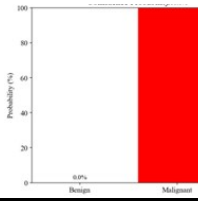

Table 7 above shows the input medical images and the highlighted tumor regions in the table that show the status of the cancer by the model. It also presents the respective confidences probability values, which are the quantification of the confidence of the model of detecting the presence of liver cancer in each image.

Table 8: Non-Cancerous Image detection in the liver with confidence probability

No Cancer Affect		
Input Image	**Tumor Highlight/ Cancer Status**	**Confidence Probability (100%)**
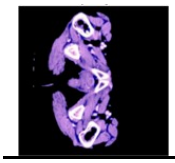	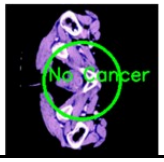	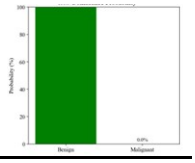

The table 8 above shows the identified liver images with no cancerous tumor areas after analyzing the images with the proposed model. It also contains the probability values of confidence, which means the model is sure of applying the images as non-cancerous cases.

4.2.1 Model Prediction and Visualization of Tumors Region with Grad-CAM

This section will show the model prediction as well as Grad-CAM heatmap and visualization of features to point at the significant areas that have a bearing on the classification of liver tumors.

Table 9: Modeling Prediction, Grad-CAM Heatmap, and feature visualization of Liver Tumor

Image	Input Image	Prediction Confidence (100.00 %)	Grad-CAM Heatmap	Feature Visualization
1	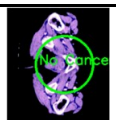	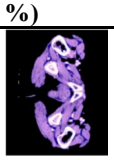		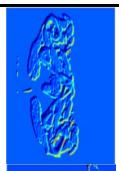
2	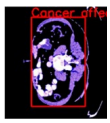	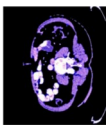	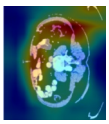	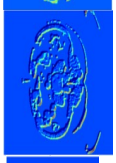
3	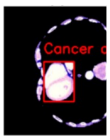	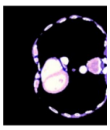	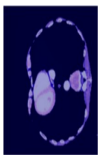	

The table 9 above shows the results of the analysis of liver CT images such as input image, prediction confidence score, the visualization of Grad-CAM heatmap, and the visualization of extracted features. It shows the focus of the proposed model on the significant areas of the tumor and how the model displays the characteristics that are used to classify the cancerous and the normal liver images.

Table10: Comparative Performance of the Current Approaches and the Proposed Modified DCNN (VGG19) to Classify Liver Tumors

Method / Metrics	Accuracy (%)	Precision (%)	Recall (%)	F1-Score (%)	Specificity (%)
GAN [17]	90.40	89.70	88.90	89.30	87.50
ResUNet [19]	92.10	91.50	90.80	91.10	89.60
EfficientNet [25]	94.30	93.80	92.90	93.30	91.40
MSFFE-Net [27]	95.60	94.90	94.20	94.50	92.80
InceptionV4 [30]	96.40	95.80	95.10	95.40	93.20
Proposed Algorithm (Modified DCNN with	97.70	97.00	96.30	95.80	94.10

VGG19
)

Table 10 above would be used to compare the performance of different existing DL models and the proposed Modified DCNN based on VGG19 architecture in classifying liver tumors. It is assessed by the main metrics of accuracy, precision, recall, F1-score, and specificity that prove that the proposed method can be used in classification with high performance.

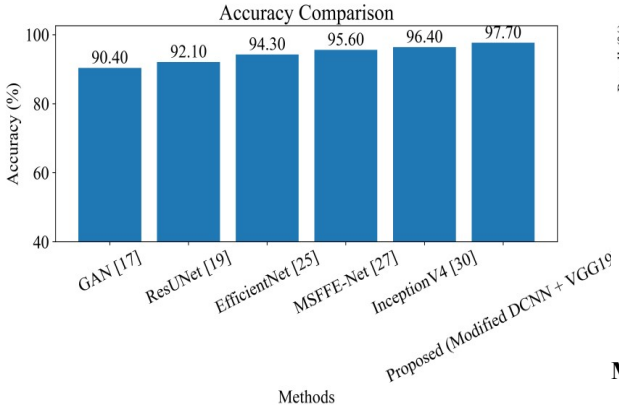

Figure 9: Comparison of Liver Tumor Classification Methods Accuracy

Above figure 9 is the accuracy performance of various liver tumor classification techniques namely GAN, ResUNet, EfficientNet, MSFFE- Net, InceptionV4, and the proposed Modified DCNN with VGG19. The classification methods are represented in the X-axis and the accuracy (%) Y-axis reflects the way, the proposed method is able to attain the highest accuracy due to the enhancement of feature learning and classification ability.

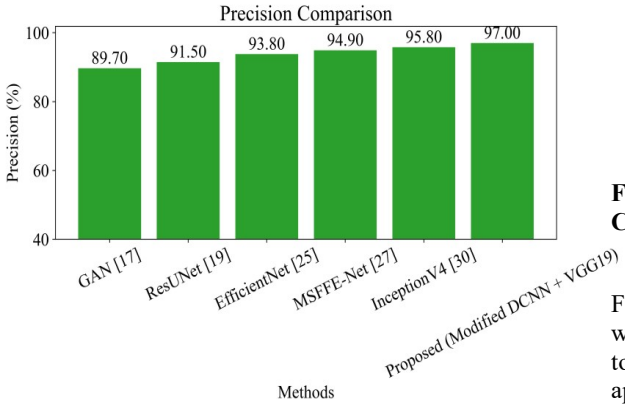

Figure 10: Accuracy Comparison of Liver Tumor Classifications Techniques

In above figure 10 shows the approximations of different DL models in the process of classifying liver tumors, which can be used to identify positive tumor cases with the help of each of the methods. The X-axis plotted the compared algorithms, and the Y-axis displays the precisions (%) of the proposed algorithms, is pointing out that the proposed Modified DCNN with VGG19 yields a higher precision with less false positive results.

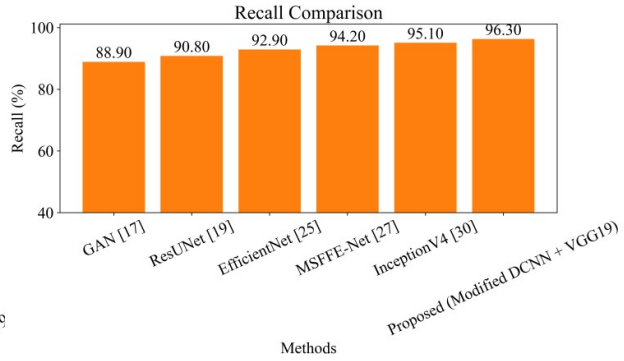

Figure 11: Liver Tumor Classification Method Recall Comparison

In the figure 11 above demonstrates the recall performance of various models, which is the extent to which each algorithm can identify real cases of tumor using the dataset. X-axis shows the methods of classification, and Y-axis shows the recall rate (%), that is, the proposed model enhances tumor detection sensitivity by reducing instances of a false negative.

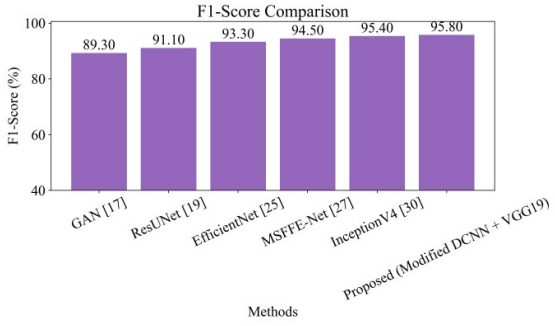

Figure 12: Comparison of Liver Tumor Classification Methods F1-score

Figure 12 above compares the values of F1-Score of various classification models, which weighs both the recall and precision when it comes to assessing the overall performance. The methods applied are presented in the X-axis and F1-Score (%) is presented in the Y-axis because it can be seen that the proposed Modified DCNN with VGG19 has a better balanced classification performance.

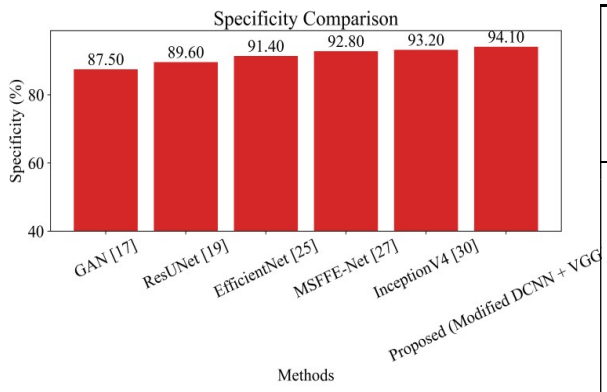

Figure 13: Specificity Comparison of Liver Tumor Classification Methods

In figure 13 above represent the specificity values of the compared methods, which are the measurements of how well each model can identify cases of non-tumor correctly. The various algorithms are used by the X-axis and the specificity (%) is used by the Y-axis, which indicates that the proposed model is effective in terms of minimizing false alarm and enhancing the quality of liver tumor identification.

5. Discussion

The findings of the experiment indicate that the proposed framework consisting of radiomics feature extraction, the FFBS algorithm, and a Modified DCNN with VGG19 model helps to significantly increase the liver tumor detection. The FFBS method allows obtaining more useful features and removing redundant ones, increasing the efficiency of classification and lowering the complexity of computations. The model has an increased accuracy, precision, recall, and F1-score than the current methods, thus it has an enhanced tumor detection ability. Also, Grad-CAM visualization enhances interpretability, as important tumor regions are highlighted, which helps to make reliable and clinically significant diagnosis.

Table 11: Ablation Study Comparison of Feature extraction and classification performance to previous methods of liver tumor segmentation

Research / Method	Feature Extraction	Classification / Model	Accuracy (%)	Key Novelty / Remarks
Hossain (2026) [25]	Multi-scale feature fusion with hybrid spatial-channel attention	UNet-based CNN	93.20	Precise liver & tumor segmentation
Bal et al. (2026) [26]	Dynamic deformable dual-pathway + embedded handcrafted features	3D CNN	94.10	Robust volumetric CT tumor segmentation
Ma et al. (2026) [27]	Multi-scale spatial-frequency feature enhancement	CNN	94.50	Spatial-frequency fusion for better tumor delineation
Gowda & Manjunath (2025) [28]	UNet70 feature maps	CNN classifier	92.80	Automatic liver tumor classification
Arora et al. (2025) [29]	Transfer learning features	DL (SegNet / VGG variant)	93.70	Used deep & TL for veins and tumors
Proposed Method (FFBS)	FFBS: Fine-grained boundary & shape-sensitive features	–	95.40	Novel feature extraction outperforming prior approaches
Proposed Method (DCNN with VGG19)	--	DCNN with VGG19	97.70	End-to-end pipeline; preserves structural & spectral features; highest accuracy among

	compared methods

Table 11 above shows a comparison between the proposed FFBS feature extraction and DCNN with VGG19 classification and earlier liver tumor segmentation methods. It underlines the excellence of the specified method, with the feature extraction and end-to-end classification accuracy of 95.40% and 97.70%, respectively, which surpasses all the prior research.

5. Conclusion

This research provides a successful model of automated detection and classification of liver tumor based on the radiomics feature extraction and DL. The proposed method will start with the radiomics feature extraction of the CT images of the liver and the application of FFBS algorithm to filter out all the redundant and irrelevant features and the most informative features. This is an optimized set of features that boosts computational efficiency and increases performance of classification. The identified features are then given to a Modified DCNN in terms of VGG19 architecture, which actually learns discriminatory patterns in terms of tumor texture, shape, and intensity. The results of the experiments prove that the offered method performs better than other methods currently applied in terms of accuracy, precision, recall, F1-score, and specificity. Also, Grad-CAM visualization enhances interpretability of models by reflecting on key tumor locations that determine predictions. Comprehensively, the proposed framework is a good and efficient model to be used in the future to support automated liver tumor diagnosis in medical imaging reports, that is, it can be expanded with multicenter larger datasets and multimodal images data in the form of MRI and PET scans. Additionally, other polishing steps can be done by incorporating new transformer-based architectures and hybrid radiomics DL systems to achieve better detection and clinical performance.

Reference

1. Chen, M., Zhang, B., Topatana, W., Cao, J., Zhu, H., Juengpanich, S., ...&Cai, X. (2020). Classification and mutation prediction based on histopathology H&E images in liver cancer using deep learning. NPJ precision oncology, 4(1), 14.https://doi.org/10.1038/s41698-020-0120-3
2. Kalaiselvi, P., &Anusuya, S. (2023). Liver tumor prediction with advanced attention mechanisms integrated into a depth-based variant search algorithm. Computers, Materials & Continua, 77(1), 1209–1226. https://doi.org/10.32604/cmc.2023.040264
3. Wang, G., Liu, D., Al-Masri, T. M., Otto, C. C., Siveke, J., Lang, S. A., Ulmer, T. F., OldeDamink, S. W. M., Luedde, T., Dahl, E., Neumann, U. P., Heij, L. R., &Bednarsch, J. (2025). Body composition in cholangiocarcinoma affects immune cell populations in the tumor and normal liver parenchyma. Journal of Clinical and Experimental Hepatology, 15(2), 102460. https://doi.org/10.1016/j.jceh.2024.102460
4. Montalvo-Romeral, V., Jauze, L., Perrot, G., Amaouche, M., Gardin, A., Aguilar González, A., Leblond, A., Zitoun-Ardon, C., Evrard, F., Cosette, J., Tatout, C., Bordier, F., Bertil-Froidevaux, E., Georger, C., van Wittenberghe, L., Paradis, V., Gay, S., Dujardin, F., Maillot, F., Gautier-Stein, A., Mithieux, G., Malfatti, E., Mussini, C., Labrune, P., Mayeuf-Louchart, A., Ronzitti, G., & Rajas, F. (2026). Enhanced lysosomal glycogen breakdown is associated with liver tumorigenesis in glycogen storage disease type III. JHEP Reports, 8(3), 101702. https://doi.org/10.1016/j.jhepr.2025.101702
5. Chen, M.-F., Ho, M.-C., Kao, J.-H., Hwang, R.-M., Deng, S.-B., Yen, K.-C., Liang, P.-C., & Wu, C.-H. (2024). Comparison of CT and gadoxetic acid–enhanced MRI with liver imaging reporting and data system to assess liver tumors before resection. Journal of the Formosan Medical Association, 123(3), 318–324. https://doi.org/10.1016/j.jfma.2023.11.008
6. Kolli, S., Parvathala, B. R., & Praveen Krishna, A. V. (2024). A novel liver tumor classification using improved probabilistic neural networks with Bayesian optimization. e-Prime – Advances in Electrical Engineering, Electronics and Energy, 8, 100514. https://doi.org/10.1016/j.prime.2024.100514
7. Troiano, M., Grignaffini, F., De Stefanis, C., D'Oria, V., Bianchi, M., Mangini, F., Francalanci, P., Alaggio, R., Frezza, F., &Alisi, A. (2025). Comparison between two artificial intelligence models to discriminate cancerous cell nuclei based on confocal fluorescence imaging in hepatocellular carcinoma. Digestive and Liver Disease, 57(5), 1015–1020. https://doi.org/10.1016/j.dld.2024.11.026
8. Ma, J., Lin, B., & Ma, Z. (2025). Dual branch multi-scale feature fusion method

for liver tumor detection. Array, 28, 100545. https://doi.org/10.1016/j.array.2025.100545

9. Zhou, B., Yuan, R., Lu, X., Chen, W., Hu, S., Xue, Y., & Yang, R. (2026). Label-free immunosensor based on magnetic nanohydrogel particle CoFe2O4@SA-Lu for detection of multiple tumor markers in liver cancer. Microchemical Journal, 220, 116350. https://doi.org/10.1016/j.microc.2025.116350
10. Balaguer-Montero, M., Morales, A. M., Ligero, M., Zatse, C., Leiva, D., Atlagich, L. M., Staikoglou, N., Viaplana, C., Monreal, C., Mateo, J., Hernando, J., García-Álvarez, A., Salvà, F., Capdevila, J., Elez, E., Dienstmann, R., Garralda, E., & Perez-Lopez, R. (2025). A CT-based deep learning-driven tool for automatic liver tumor detection and delineation in patients with cancer. Cell Reports Medicine, 6(4), 102032. https://doi.org/10.1016/j.xcrm.2025.102032
11. Ding, Q., Liu, J., Zhang, X., Li, J., Wong, K. M.-C., Sharma, A., Zhang, P., Fan, Q., Yin, C., Zhou, H., James, T. D., & Kim, J. S. (2025). A versatile NIR probe for multifunctional detection of tumors, fatty liver, and liver injury. Chemical Science, 16(27), 12408–12415. https://doi.org/10.1039/d5sc01433f
12. Kaur, J., &Kaur, P. (2024). PSO-PSP-Net + InceptionV3: An optimized hyper-parameter tuned computer-aided diagnostic model for liver tumor detection using CT scan slices. Biomedical Signal Processing and Control, 95(Part B), 106442. https://doi.org/10.1016/j.bspc.2024.106442
13. Ma, J., Ouyang, K., Ma, Z., Xia, M., Xu, S., & Lu, K. (2024). Transformer dense center network for liver tumor detection. Biomedical Signal Processing and Control, 91, 106066. https://doi.org/10.1016/j.bspc.2024.106066
14. Kan, F., Jin, F., Mylonas, A., Zwan, B., Nguyen, T., Moodie, T., Hardcastle, N., Ramachandran, P., Mason, D., Wang, T., Lee, Y. Y., Keall, P., &Sengupta, C. (2025). Deep learning-based framework for liver tumour motion detection using fiducial markers in kilovoltage X-ray images. Radiotherapy and Oncology, 206(Supplement 1), S3215–S3217. https://doi.org/10.1016/S0167-8140(25)00260-9
15. Ma, L., Li, J., Azamuddin, M., Zheng, S., Wang, W., & Wang, P. (2022). Detection of tumour boundary in metastatic liver disease with 2D multibreath-hold susceptibility-weighted imaging. Magnetic Resonance Imaging, 92, 26–32. https://doi.org/10.1016/j.mri.2022.05.011
16. Shi, J., Qin, W., Lin, Y., Li, M., Wu, Y., Luo, H., Yan, J., Huang, K.-J., & Tan, X. (2023). Enhancing biosensingwith fourfold amplification and self-powering capabilities: MoS2@C hollow nanorods-mediated DNA hexahedral framework architecture for amol-level liver cancer tumor marker detection. AnalyticaChimicaActa, 1271, 341413. https://doi.org/10.1016/j.aca.2023.341413
17. Zhao, J., Li, D., Xiao, X., Accorsi, F., Marshall, H., Cossetto, T., Kim, D., McCarthy, D., Dawson, C., Knezevic, S., Chen, B., & Li, S. (2021). United adversarial learning for liver tumor segmentation and detection of multi-modality non-contrast MRI. Medical Image Analysis, 73, 102154. https://doi.org/10.1016/j.media.2021.102154
18. Yang, T.-L., Tsai, H.-W., Huang, W.-C., Lin, J.-C., Liao, J.-B., Chow, N.-H., & Chung, P.-C. (2022). Pathologic liver tumor detection using feature aligned multi-scale convolutional network. Artificial Intelligence in Medicine, 125, 102244. https://doi.org/10.1016/j.artmed.2022.102244
19. Aslam, M. S., Younas, M., Sarwar, M. U., Shah, M. A., Khan, A., Uddin, M. I., Ahmad, S., Firdausi, M., &Zaindin, M. (2021). Liver-tumor detection using CNN ResUNet. Computers, Materials and Continua, 67(2), 1899–1914. https://doi.org/10.32604/cmc.2021.015151
20. Kose, E., Kahramangil, B., Aydin, H., Donmez, M., Takahashi, H., Acevedo-Moreno, L.-A., Sasaki, K., Aucejo, F., & Berber, E. (2020). A comparison of indocyanine green fluorescence and laparoscopic ultrasound for detection of liver tumors. HPB, 22(5), 764–769. https://doi.org/10.1016/j.hpb.2019.10.005
21. Abdelrahim, M., Esmail, A., Saharia, A., He, A., Dhani, H., Aushev, V., Jurdi, A., Starr, J., & Gauthier, P. (2022). The feasibility of tumor recurrence detection in liver post-transplantation for patients with hepatocellular carcinoma via personalized, tumor-informed ctDNA testing. Annals of

Oncology, 33(Supplement 4), S308–S309. https://doi.org/10.1016/j.annonc.2022.04.255

22. Jameel, R., & Amin, J. (2026). Unified classification and segmentation of liver tumors using shifted window transformer networks with incremental learning. Biomedical Signal Processing and Control, 114, 109318. https://doi.org/10.1016/j.bspc.2025.109318
23. Wu, W., Mao, L., Wang, M., Li, L., & Xi, X. (2026). FFK-net: A feature fusion-based Kolmogorov–Arnold network for liver tumor segmentation. Neurocomputing, 133214. https://doi.org/10.1016/j.neucom.2026.133214
24. Spinczyk, D., Rosiak, G., Żyłkowski, J., Milczarek, K., Konecki, D., Zaczkowski, K., Tomaszewska, A., Przepióra, Ł., Wolińska-Sołtys, A., Sperka, P., Hajda, D., &Piętka, E. (2026). Initial evaluation of a mixed-reality system for image-guided navigation during percutaneous liver tumor ablation. Computerized Medical Imaging and Graphics, 128, 102714. https://doi.org/10.1016/j.compmedimag.2026.102714
25. Hossain, J. (2026). EfficientNet-based multi-scale feature fusion with hybrid spatial-channel attention for precise liver and tumor segmentation in CT scans. Journal of Liver Transplantation, 22, 100331. https://doi.org/10.1016/j.liver.2026.100331
26. Bal, N. P., Bal, A., Kolya, A. K., Bhattacharyya, S., Ekbal, A., & Sharma, P. (2026). D33D-net: A robust dynamic deformable dual-pathway 3D deep neural network with embedded handcrafted features for liver tumor segmentation in CT images. Applied Soft Computing, 114891. https://doi.org/10.1016/j.asoc.2026.114891
27. Ma, J., Zhang, K., Ma, Z., & Lu, K. (2026). MSFFE-Net: Multi-scale spatial-frequency feature enhancement for accurate liver tumor segmentation. Biomedical Signal Processing and Control, 113(Part A), 108963. https://doi.org/10.1016/j.bspc.2025.108963
28. Gowda, Y. N., &Manjunath, R. V. (2025). Automatic liver tumor classification using UNet70: A DL model. Journal of Liver Transplantation, 18, 100260. https://doi.org/10.1016/j.liver.2025.100260
29. Arora, A., Jordar, R., Jena, J. J., Singh, S., Patra, S. S., &Gourisaria, M. K. (2025). Harnessing DL and transfer learning models for segmentation of liver tumors and veins. Procedia Computer Science, 259, 1874–1882. https://doi.org/10.1016/j.procs.2025.04.143
30. Rahman, H., Ben Aoun, N., Bukht, T. F. N., Ahmad, S., Tadeusiewicz, R., Pławiak, P., &Hammad, M. (2025). Automatic liver tumor segmentation of CT and MRI volumes using ensemble ResUNet-InceptionV4 model. Information Sciences, 704, 121966. https://doi.org/10.1016/j.ins.2025.121966